Geophys. J. R. astr. Soc. (1984) **79**, 705–725

Correlation of porosity and permeability of reservoirs with well oscillations induced by earth tides

L. W. Morland *School of Mathematics and Physics, University of East Anglia, Norwich NR4 7TJ*

E. C. Donaldson* *US Department of Energy, Bartlesville Energy Technology Center, Bartlesville, Oklahoma, USA*

Received 1984 January 14

Summary. Periodic gravity perturbations, known as earth tides, produce minute expansions and contractions of subsurface geologic formations. The motions induce water level oscillations in wells connected to the deep reservoirs, and a measurable phase lag occurs between the maximum gravity and the maximum water level. The amplitude of the water level oscillations induced by the small harmonic gravity variations of the earth tides and the phase lag relative to the tide are related to the reservoir porosity and permeability.

The motions of an elastic subsurface reservoir are analysed by considering an axially symmetric system of finite volume which is activated by oscillations of a rigid rock mass overlying the reservoir. The geometric parameters involved are the thickness of the reservoir, radial extent, depth and fluid level in the well. The physical parameters for which data are available or satisfactory estimates can be made are the fluid viscosity, densities, temperature, compressibilities and shear modulus. These properties refer to *in situ* conditions at large overburden pressure. Permeability and porosity at *in situ* conditions are not directly measurable, and methods of indirect estimation are of practical interest. This analysis correlates these two parameters with the amplitude and phase lag of the induced well fluid oscillation.

For the very small strains and fluid volume fraction changes induced by the tides, slow flow of a viscous fluid through an isotropic porous matrix is assumed. An axially-symmetric analysis for a uniform permeable layer perturbed by the oscillations of the rigid overburden rock yields explicit expressions for the oscillation amplitude and phase in the well. Selected results from numerical solutions having a wide range of realistic parameter values are presented. The results clearly show the dependence of amplitude and phase lag on the dimensionless permeability, and the near proportionality of the amplitude on the reciprocal of the porosity (porosity has no other significant influence). Finally, it is shown how asymptotic approximations of

*Now in Petroleum Engineering Department, University of Oklahoma, Norman, Oklahoma, USA.

the direct solution allow an inversion which determines the permeability and porosity in terms of the amplitude and phase lag, given the other reservoir properties.

1 Introduction

The fluid level of a well connected to a subsurface fluid reservoir responds to the semi-diurnal and diurnal tides in two readily measurable modes, phase lag and water level variation. Dilation and compression of the reservoir occurs on a periodic basis in step with the changes of gravity. The resulting periodic fluctuations of the fluid level in the well are out of phase with the changes in gravity due to resistance of the reservoir to the flow of fluid into and out of the well bore (Fig. 1). The amplitude of the water level fluctuation is related to the porosity of the reservoir. Although the relative gravity variation in earth tides does not exceed a magnitude of 10^{-7}, it has a significant effect on ground fluid flow, as noted in earlier reviews (Sperling 1953; Rinehart 1972, 1976; Melchoir 1983; Robinson & Bell 1971; Marine 1975). The oscillation amplitude and phase lag relative to the tide provide two independent quantities that can be determined accurately. We present a correlation of these two well motion parameters with *in situ* parameters describing the reservoir properties, and in particular their strong dependence on the permeability and volume fraction of fluid in the reservoir matrix. Explicit estimates of reservoir permeability and fluid volume fraction are derived in terms of these measurable well parameters.

Rinehart (1975) proposed a simple mechanism of a rigid impermeable rock mass oscillating vertically with the earth tide and perturbing the matrix and fluid of an underlying permeable reservoir, which in turn produces an oscillating volume flux in and out of a penetrating well. The very small amplitude overburden oscillation over a sufficiently large area produces sufficient lateral flux to induce a measurable oscillation of the fluid level in the well. Since the matrix strains, changes of fluid volume fraction, and velocities, accompanying the oscillatory motion are extremely small, it is appropriate to model the oscillatory motion, superimposed on the static stress-strain fields defined by the mean gravity configuration, as slow linearly viscous flow through a porous linearly elastic matrix. Assuming isotropy, a matrix-fluid mixture theory (Morland 1978) involves a mixture shear modulus and four mixture compressibilities, the fluid viscosity, the matrix permeability, and the volume fraction of fluid. Plane and axially symmetric flow analyses for a deep reservoir of large lateral extent, uniform in thickness and properties, have been presented by Morland (1977), where the magnitude of the well oscillation was estimated to demonstrate that it could reach a measurable size. We now extend and refine the axially symmetric analysis to

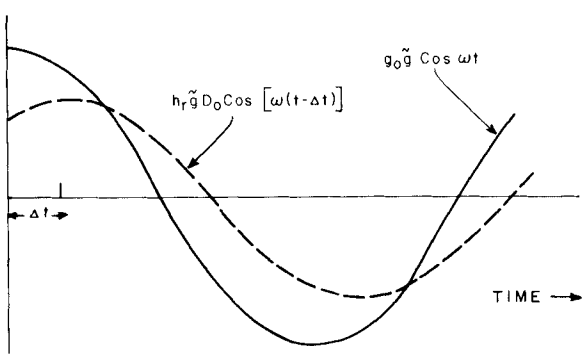

Figure 1. Gravity variation (——) and well level fluctuation (– – –) showing phase lag Δt.

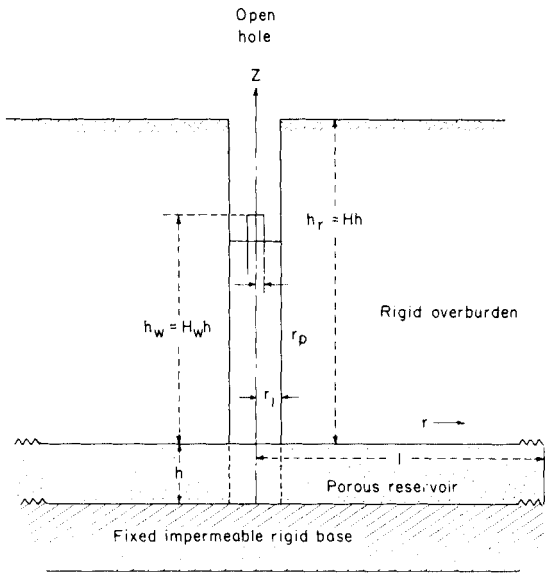

Figure 2. Axially-symmetric well-reservoir geometry with reference to cylindrical polar coordinates (r, θ, z).

determine explicit expressions for both amplitude and phase lag in terms of the *in situ* reservoir parameters, and in particular to highlight the influence of fluid volume fraction and matrix permeability. Asymptotic approximations with wide validity yield an inverse solution which estimates the permeability and fluid volume fraction in terms of the amplitude and phase lag, given the other reservoir properties.

Fig. 2 shows the axially symmetric well-reservoir geometry with reference to cylindrical polar coordinates (r, θ, z), and the reservoir motion in the matrix-fluid layer $r_1 \leqslant r \leqslant l$, $-h \leqslant z \leqslant 0$, is assumed to depend only on r, z and time t, independent of θ. The base $z = -h$ and outer wall $r = l$ are rigid, fixed and impermeable, and the upper boundary $z = 0$ $(r_1 \leqslant r \leqslant l)$ is rigid and impermeable, but oscillates due to the earth tide influence on the overburden rock. It is supposed that any vertical drag from the far field overburden is negligible so that the vertical overburden motion between $r = r_1$ and $r = l$ is due solely to the gravity variation and reservoir pressure perturbation on $z = 0$ $(r_1 \leqslant r \leqslant l)$. This assumption and the fixed base assumption, reflecting Rinehart's (1975) proposal, are idealizations which may not be realized, but at present we have no evidence for alternative boundary conditions. The approximation of rigid overburden and rigid basement is an assumption that the strain increment induced by gravity variation in these regions is much smaller than the strain increment in the reservoir matrix or the dilatation increment in the reservoir fluid. That is, we suppose that the reservoir matrix of fluid is much more compressible than the surrounding rock. The assumption of a fixed basement, however, lacks strong physical justification. The well-matrix interface $r = r_1$ is supposed open to simplify the interface conditions, which are then simply balances between the well fluid pressure and matrix and reservoir fluid normal pressures without the introduction of an unknown casing interaction pressure. The latter may be significant in many practical situations, but will require a more difficult analysis.

The earth tide effect is restricted to a vertical gravity variation

$$g = g_0(1 + \tilde{g}\cos\omega t) = g_0 + \mathrm{Re}[g_0\tilde{g}\exp(i\omega t)], \tag{1}$$

where for half-day and day tides $\omega = 1.454 \times 10^{-4}\,\mathrm{s}^{-1}$ and $\omega = 0.727 \times 10^{-4}\,\mathrm{s}^{-1}$, $\tilde{g} = 0\,(10^{-7})$

(Rinehart 1975). If the oscillatory displacement of the well fluid level is d (in the z-direction), then setting

$$d = h_r \tilde{g} D_0 \cos[\omega(t-\Delta t)] = h_r \tilde{g} D_0 \operatorname{Re}[\![\exp[i\omega(t-\Delta t)]]\!], \tag{2}$$

where h_r is the overburden depth, introduces a dimensionless complex displacement

$$D = D_0 \exp(-i\omega\Delta t) \tag{3}$$

such that $\omega\Delta t = \tau$ defines the phase lag. For $\tilde{g} = 10^{-7}$, $h_r = 10^3$ m, the oscillation amplitude is $10^{-2} D_0$ cm, so that D_0 of order 10^2 is required for $d = 0$ (1 cm). Dimensionless well radius R_1, top pipe radius R_p if the well is packed, reservoir radius L, overburden depth H, and mean well fluid level H_W, are defined relative to the layer thickness h by

$$r_1 = hR_1, \quad r_p = hR_p, \quad l = hL, \quad h_r = hH, \quad h_W = hH_W, \tag{4}$$

and Morland's (1977) solution requires the strong inequalities

$$L \gg 1, \quad H \geqslant H_W \gg 1, \tag{5}$$

which are common in practical situations.

Phase lag depends primarily on the drag between fluid and matrix, and hence on the fluid viscosity μ and matrix permeability k. The extension and refinement of Morland's (1977) analysis shows that μ, k and ω, enter the solution only through a dimensionless reciprocal permeability

$$n = \frac{\bar{k}}{k}, \quad \bar{k} = \frac{\mu\omega r_p^2}{\rho_f g_0 h}, \tag{6}$$

where ρ_f is the fluid density. It is shown that the combination of significant amplitude D_0 and significant phase lag τ ($\gtrsim 11^\circ$) requires n to lie in an approximate range

$$0.04 \lesssim n \lesssim 0.2, \tag{7}$$

with the lower limit (upper limit of k) required for significant phase lag and the upper limit (lower limit of k) required for significant amplitude. Since μ can increase by a factor of 100 from water through light to heavy oils, the corresponding range of k to satisfy (7) differs widely between fluids. However, the ratio μ/k which defines a reciprocal drag coefficient (dimensional) in Darcy's law is determined by n for given ω, r_p, ρ_f and h. A range of $\bar{k}$ for the half-day tide, $\omega \approx 1.5 \times 10^{-4}\,\mathrm{s}^{-1}$, with $h = 10$ m, $r_p = r_1 = 0.1$ m, $\rho_f = 10^3\,\mathrm{kg\,m}^{-3}$, is 0.6×10^{-14}–$0.6 \times 10^{-12}\,\mathrm{m}^2$ for $\mu \approx 0.4 \times 10^{-3}$ Pa s (water) to 0.4×10^{-1} Pa s (heavy oil), which at $n = 0.1$ corresponds to a range of k from 0.6×10^{-13} to $0.6 \times 10^{-11}\,\mathrm{m}^2$. For a packed well with smaller r_p, $\bar{k}$ decreases, and hence the corresponding k decreases at given n.

It is also shown that the phase lag is not significantly affected by a change of the mean fluid volume fraction ϕ_0, nor is the product $\phi_0 D_0$, so that the amplitude D_0 is essentially proportional to the reciprocal of ϕ_0, and a significant amplitude requires small ϕ_0. This general conclusion was deduced in the previous magnitude estimates (Morland 1977), but the inference there, without analysis, that the amplitude is also proportional to r_1^2/r_p^2, and hence increased signficantly by packing the well and introducing a pipe of small radius, is not correct. The present analysis shows that r_p enters only through the parameter n and has little influence on the amplitude once it attains a significant size. The magnitude estimate for D_0 depends also on the relative magnitudes of the four compressibilities associated with the matrix-fluid mixture. Before analysing the formal solution we discuss the reservoir

elasticity in terms of the compressibilities used in Morland (1977) and in terms of an alternative set more common in petroleum engineering (Amyx, Bass & Whiting 1960).

Previous correlations of earth tide effects on well fluid with reservoir properties by Bredehoeft (1967), Bodvarsson (1970), Robinson & Bell (1971) and Rhoads & Robinson (1979) follow an analysis of well pressure variations due, for example, to seismic disturbances given by Cooper *et al.* (1965). In all these treatments the reservoir is described by its porosity, fluid bulk modulus, and an overall bulk modulus, and permeability does not appear explicitly. Our analysis incorporates the permeability, four independent compressibilities, and the matrix shear modulus. The shear modulus is shown to have a significant role in the axisymmetric balances, and a significant well fluid oscillation has implications for the relative magnitudes of the four compressibilities. Furthermore, the above analyses start from assumed dilatations inferred from gravity tide effects on a homogeneous elastic earth; that is, there is no solution for the matrix deformation and fluid flow induced by the gravity variation. A given gravity variation (tidal stress distribution) must induce very different deformation in the reservoir if it has distinct elastic properties from the surrounding rock. Here we have adopted the limit case of rigid surround, but treat the full mass and momentum balances for the permeable elastic matrix and compressible fluid under a prescribed vertical gravity oscillation. We have not included possible effects of any horizontal component of the gravity tide, and cannot assess what influence it would have on the well fluid motion. Our conclusions, therefore, must be regarded as specific to the particular boundary conditions and gravity variation. However, the analysis has demonstrated the influence of reservoir elasticity and permeability on oscillations induced in a connected well, and the mixture theory provides the framework for alternative formulations of gravity tide effects.

2 Reservoir elasticity

We suppose that the very small matrix strains and very small change in fluid volume fraction induced by the earth tides are described by linear isotropic elastic matrix relations with constant moduli, a fluid pressure–dilatation law with constant compressibility, and a porosity variation relation linear in the matrix and fluid partial pressures. All the constant coefficients define properties at the *in situ* conditions. The term porosity is used to denote the fluid volume fraction, and the term matrix to denote the structured solid-void medium containing the fluid. Thus the matrix is not necessarily fluid saturated, but the solid-void structure is treated as a single constituent of the mixture. Let the intrinsic compressibility of this matrix be κ_s, and that of the fluid κ_f, measured at *in situ* conditions. Adopting the mixture theory developed by Morland (1972, 1975, 1978), if p^s and p^f are the partial pressure increments from the equilibrium (mean gravity) conditions, and ϕ is the porosity with equilibrium value ϕ_0, then

$$\phi = \phi_0(1 - ap^s + bp^f), \tag{8}$$

where a and b are positive constants whose magnitudes are of compressibility order. A relative porosity change $(\phi-\phi_0)/\phi_0$ is therefore of infinitesimal strain order.

It is assumed that the mean area fraction of fluid across an arbitrary mixture plane is also ϕ, and so $1-\phi$ is the area fraction of matrix. Hence the partial and intrinsic (pore pressure) fluid pressures p_f and ${}^E p^f$, and partial and intrinsic matrix stresses $\boldsymbol{\sigma}^s$ and ${}^E\boldsymbol{\sigma}^s$, are related by

$$p^f = \phi_0\, {}^E p^f, \quad \boldsymbol{\sigma}^s = (1-\phi_0)\, {}^E\boldsymbol{\sigma}^s, \tag{9}$$

where ϕ is evaluated as the mean value ϕ_0 in view of the infinitesimal changes. Further, the partial and intrinsic infinitesimal dilatations ϵ and ${}^{\mathrm{E}}\epsilon$ are related by

$$ {}^{\mathrm{E}}\epsilon^{\mathrm{f}} = \epsilon^{\mathrm{f}} + \frac{\phi-\phi_0}{\phi_0}, \quad {}^{\mathrm{E}}\epsilon^{\mathrm{s}} = \epsilon^{\mathrm{s}} - \frac{\phi-\phi_0}{1-\phi_0}, \tag{10} $$

where the partial dilatations are given by the respective trace of the mean constituent displacement fields viewed as continuous fields over the mixture region. The intrinsic compression relations are

$$ {}^{\mathrm{E}}\epsilon^{\mathrm{f}} = -\kappa_{\mathrm{f}}\,{}^{\mathrm{E}}p^{\mathrm{f}}, \quad {}^{\mathrm{E}}\epsilon^{\mathrm{s}} = -\kappa_{\mathrm{s}}\,{}^{\mathrm{E}}p^{\mathrm{s}}, \tag{11} $$

and the mixture deviatoric stress-strain relation has a modulus G. By (8), (9), (10) and (11), the partial pressure-dilatation relations become (Morland 1978)

$$ -p^{\mathrm{s}} = c_{11}\,\epsilon^{\mathrm{s}} + c_{12}\,\epsilon^{\mathrm{f}}, \quad -p^{\mathrm{f}} = c_{21}\epsilon^{\mathrm{s}} + c_{22}\epsilon^{\mathrm{f}}, \tag{12} $$

where

$$ \Delta \begin{pmatrix} c_{11} & c_{12} \\ c_{21} & c_{22} \end{pmatrix} = \begin{pmatrix} (1-\phi_0)(\kappa_{\mathrm{f}} + \phi_0 b) & \phi_0^2 b \\ \phi_0(1-\phi_0)a & \phi_0(\kappa_{\mathrm{s}} + \phi_0 a) \end{pmatrix}, \tag{13} $$

$$ \Delta = \kappa_{\mathrm{s}}\kappa_{\mathrm{f}} + \phi_0(\kappa_{\mathrm{s}} b + \kappa_{\mathrm{f}} a). \tag{14} $$

Rejecting the symmetry relation $c_{21} = c_{12}$ (until confirmed by tests for the given mixture), there are four mixture compressibilities c_{ij} $(i, j = 1, 2)$ and a shear modulus G. The coefficients a and b can be eliminated in terms of two mixture compressibilities. A jacketed test which allows the pore fluid to drain at constant intrinsic fluid pressure, that associated with *in situ* reservoir conditions, determines the bulk compressibility (Biot & Willis 1957; Geertsma 1957; Amyx *et al.* 1960) κ_{b}. Thus the intrinsic pressure increment ${}^{\mathrm{E}}p^{\mathrm{f}} = 0$, which in turn implies ${}^{\mathrm{E}}\epsilon^{\mathrm{f}} = 0$ and $p^{\mathrm{f}} = 0$ (when $\kappa_{\mathrm{f}} \neq 0$), so that

$$ \kappa_{\mathrm{b}} = -\left.\frac{\partial \epsilon^{\mathrm{s}}}{\partial p^{\mathrm{s}}}\right|_{p^{\mathrm{f}}}, \tag{15} $$

denoted κ by Morland (1978). From (12), (13), (14).

$$ \kappa_{\mathrm{b}} = \frac{c_{22}}{c_{22}c_{11} - c_{12}c_{21}} = \frac{\kappa_{\mathrm{s}} + \phi_0 a}{1-\phi_0}. \tag{16} $$

In an unjacketed test the pore pressure is the same as the confining pressure p, so that

$$ p^{\mathrm{f}} = \phi_0\,{}^{\mathrm{E}}p^{\mathrm{f}} = \phi_0 p, \quad p^{\mathrm{s}} = (1-\phi_0)p, \quad {}^{\mathrm{E}}p^{\mathrm{s}} = p, \tag{17} $$

and the unjacketed compressibility is defined by (Biot & Willis 1957)

$$ \delta = -\frac{d\epsilon^{\mathrm{s}}}{dp}, = \frac{(1-\phi_0)\,c_{22} - \phi_0 c_{12}}{c_{22}c_{11} - c_{12}c_{21}} = (1-\phi_0)\kappa_{\mathrm{b}} - \frac{\phi_0^2 b}{1-\phi_0}, \tag{18} $$

using (17), (12), (13), (14). By (16) and (18), the coefficients a and b can be expressed in terms of κ_{b}, δ, and κ_{s}. Note that the 'compressibility of the rock matrix c_{r}' introduced by Geertsma (1957) has no meaning unless $\kappa_{\mathrm{f}} = \kappa_{\mathrm{s}}$, when $c_{\mathrm{r}} = \kappa_{\mathrm{s}}$, since only then are the intrinsic dilatations of matrix and fluid identical when subjected to the same intrinsic pressure increments as required by Geertsma's definition. Morland's (1977) reservoir analysis is expressed in terms of the four compressibilities κ_{s}, κ_{f}, κ_{b}, δ. The symmetry relation $c_{21} = c_{12} \Leftrightarrow \delta = \kappa_{\mathrm{s}}$.

Two alternative mixture compressibilities (Amyx *et al.* 1960) are the formation compaction κ_p and effective rock compressibility κ_e. In a jacketed test with draining at ${}^E p^f = p^f = 0$,

$$\kappa_p = -\frac{1}{\phi V}\frac{\partial(\phi V)}{\partial p^s}\bigg|_{p^f}, \tag{19}$$

where V is a mixture element volume $V_0(1+\epsilon^s)$ with initial value V_0. Hence, by (8) and (15),

$$\kappa_p = \kappa_b + a, = \frac{\kappa_s + a}{1-\phi_0}, \tag{20}$$

by (16). In a jacketed test at constant confining matrix pressure p^s and increasing pore pressure ${}^E p^f$,

$$\kappa_e = \frac{1}{\phi V}\frac{\partial(\phi V)}{\partial {}^E p^f}\bigg|_{p^s} = \frac{1}{V}\frac{\partial(\phi V)}{\partial p^f}\bigg|_{p^s},$$

$$= \phi_0\left\{\frac{c_{12}}{c_{22}c_{11}-c_{12}c_{21}} + b\right\} = \frac{\phi_0 b}{1-\phi_0}, \tag{21}$$

using (8), (9), (12), (13), (14). Now the mixture relations can be expressed in terms of the four compressibilities $\kappa_f, \kappa_b, \kappa_p, \kappa_e$ by using the identities

$$\kappa_s = \kappa_b - \phi_0\kappa_p, \quad a = \kappa_p - \kappa_b, \quad \phi_0 b = (1-\phi_0)\kappa_e, \tag{22}$$

when (13), (14) become

$$\kappa_D\kappa_b\begin{pmatrix} c_{11} & c_{12} \\ c_{21} & c_{22}\end{pmatrix} = \begin{pmatrix} \kappa_f + (1-\phi_0)\kappa_e & \phi_0\kappa_e \\ \phi_0(\kappa_p - \kappa_b) & \phi_0\kappa_b\end{pmatrix}, \tag{23}$$

$$\kappa_D\kappa_b = (\kappa_f + \kappa_e)\kappa_b - \phi_0\kappa_p\kappa_e. \tag{24}$$

From (20) and (22),

$$\kappa_p = \frac{\kappa_b}{\phi_0}\left(1 - \frac{\kappa_s}{\kappa_b}\right), = 0\left(\frac{\kappa_b}{\phi_0}\right) \tag{25}$$

when κ_s/κ_b is not close to unity, that is, when the free draining compressibility of the saturated matrix is much higher than the intrinsic compressibility of the matrix material. In the final solution we set

$$\kappa_p = \frac{\nu\kappa_b}{\phi_0}, \quad \nu = 1 - \frac{\kappa_s}{\kappa_b} < 1, \tag{26}$$

and show that significant well oscillation amplitude requires that ϕ_0 is small and $\nu = 0(1)$, that is, $\kappa_p \gg \kappa_b$, that $G\kappa_e \gtrsim G\kappa_f \gtrsim 1$, and that κ_e is not of greater magnitude than κ_b. Since

$$\frac{\kappa_b}{\kappa_e} = \frac{a}{b} + \frac{\kappa_s}{\phi_0 b}, \tag{27}$$

and we expect p^f and p^s to have similar effects in the porosity variation (8), that is, b and a to have similar magnitudes, (27) suggests that $\kappa_b = 0(\kappa_e)$, or $\kappa_b \gg \kappa_e$ if $\kappa_s = 0(b)$ and ϕ_0 is small. The requirement of large κ_p relative to κ_b is simply a statement that fluid is squeezed out of (and into) the matrix easier than the matrix compresses (expands) under external pressure increase (decrease), which is consistent with the larger flux of fluid into the well.

These compressibility comparisons are required at the *in situ* reservoir conditions, and may not apply in low-pressure laboratory measurements.

3 Reservoir and well coupling

An axially symmetric solution of the harmonic oscillatory motion of matrix and fluid in the reservoir was presented by Morland (1977), and the analysis will not be repeated. The complex amplitude D, incorporating the real amplitude D_0 and phase lag τ, of the well oscillation is coupled to the reservoir matrix and fluid motions by flux and pressure conditions at the interface $r = r_1$, $-h \leqslant z \leqslant 0$ (Fig. 2) and the reservoir motion is linked to the overburden oscillation by a pressure-acceleration relation at the upper boundary $z = 0$, $r_1 \leqslant r \leqslant l$. The analysis is presented in terms of dimensionless complex stress and velocity amplitudes, P, Σ_{rr}, Σ_{zz}, $\mathbf{V}^{\mathrm{f}}$, $\mathbf{V}^{\mathrm{s}}$ of the oscillatory perturbation defined by

$$p^{\mathrm{f}} = -\mathrm{Re}[\rho_0 g_0 h\tilde{g} P \exp(i\omega t)], \quad (\sigma_{rr}, \sigma_{zz}) = \mathrm{Re}[\rho_0 g_0 h\tilde{g} \exp(i\omega t)(\Sigma_{rr}, \Sigma_{zz})],$$
$$(\mathbf{v}^{\mathrm{f}}, \mathbf{v}^{\mathrm{s}}) = \mathrm{Re}[i\omega\kappa_{\mathrm{b}}\rho_0 g_0 h^2\tilde{g} \exp(i\omega t)(\mathbf{V}^{\mathrm{f}}, \mathbf{V}^{\mathrm{s}})], \tag{28}$$

where ρ_0 is the equilibrium mixture density and σ_{rr}, σ_{zz} are the partial radial and vertical stresses in the matrix. On the upper boundary $z = 0$, $V_z^f = V_z^s = V$, the vertical velocity perturbation of the overburden rock. The use of V as the element volume, equations (19) and (21), is no longer required.) The boundary conditions result in four complex linear equations for D and

$$\hat{V} = \frac{2V}{H}, \quad \hat{q}_0 = \frac{2R_1}{H(L^2 - R_1^2)}(V_r^{\mathrm{f}} - V_r^{\mathrm{s}})_{R=R_1}, \quad \hat{w}_0 = \frac{2R_1}{H(L^2 - R_1^2)}(V_r^{\mathrm{f}} + V_r^{\mathrm{s}})_{R=R_1}, \tag{29}$$

where $\hat{q}_0$, $\hat{w}_0$, measure the difference and sum of radial matrix and fluid velocities at the interface.

For the purpose of correlating the well oscillation with the flux at the well–reservoir interface, it is supposed that the fluid column in the well is incompressible so that the flux is transmitted directly to the surface. Then, modifying Morland's (1977) expression to allow for packing and a pipe of radius $r_{\mathrm{p}} = hR_{\mathrm{p}}$,

$$D = -\frac{\kappa_{\mathrm{b}}\rho_0 g_0 h(L^2 - R_1^2)}{2R_{\mathrm{p}}^2}\{\hat{w}_0 - (1 - 2\phi_0)\hat{q}_0\}. \tag{30}$$

The dimensionless pressure perturbation P_{w} in the well at the interface level (averaged over the layer thickness) is

$$P_{\mathrm{w}} = -\frac{\rho_{\mathrm{ws}}}{\rho_0} H(D + Y), \quad \rho_{\mathrm{ws}} HY = \int_0^{H_{\mathrm{w}}} \rho_{\mathrm{w}}(Z)dZ + \tfrac{1}{2}\rho_{\mathrm{w0}}, \tag{31}$$

where $\rho_{\mathrm{w}}(Z)$ is the well fluid density with surface value $\rho_{\mathrm{ws}} = \rho_{\mathrm{w}}(H_{\mathrm{w}})$ and value at the layer $\rho_{\mathrm{w0}} = \rho_{\mathrm{w}}(0)$. We will adopt the approximation $\rho_{\mathrm{w}} \equiv \rho_{\mathrm{f}}$ for illustration, when $Y = (H_{\mathrm{w}} + \tfrac{1}{2})/H$; the previous solution also adopted $H_{\mathrm{w}} = H \gg \tfrac{1}{2}$, giving $Y = 1$. The open interface conditions are

$$R = R_1, \quad P = \phi_0 P_{\mathrm{w}}, \quad \Sigma_{rr} = (1 - \phi_0)P_{\mathrm{w}}. \tag{32}$$

Momentum balance for the oscillatory motion of the rigid overburden of density ρ_{r} requires

$$-\frac{2\rho_0}{\rho_{\mathrm{r}} H(L^2 - R_1^2)} \int_{R_1}^{L} R(\Sigma_{zz} + P)_{z=0} dR = 1 + \kappa_{\mathrm{b}}\rho_0 h^2 \omega^2 V, \tag{33}$$

but the final momentum term in V is negligible compared to unity. The new features are the term Y (in place of unity) in P_w (28) and the pipe radius $R_p \leqslant R_1$ entering the D expression (30). It will be shown that Y of order unity has no influence on τ or on a significant amplitude D_0, and that $R_p \ll R_1$ influences only τ.

The reservoir solution (Morland 1977) expresses the stresses P, Σ_{rr} on $R = R_1$ and P, Σ_{zz} on $z = 0$ in terms of $\hat{w}_0, \hat{q}_0, \hat{V}$ so that (30), (31), (32), (33) result in four simultaneous linear complex equations for $D, \hat{w}_0, \hat{q}_0, \hat{V}$. Kramer's rule was used to estimate the magnitude D_0 under various assumptions on the reservoir geometry and elasticity. We now present the modified four equations in terms of the alternative compressibilities κ_f, κ_b, κ_p, κ_e. The following dimensionless real parameters arise:

$$\bar{G} = \kappa_b G, \quad \hat{G} = \frac{\bar{G}(L^2 - R_1^2)K_D}{R_1^2 \phi_0 \kappa_p}, \tag{34}$$

$$M_{11} = \frac{2\phi_0 \kappa_e - (\kappa_f + \kappa_e)}{2\kappa_D} - \frac{2}{3}\bar{G}, \quad M_{12} = -M_{11} + \frac{\phi_0 \kappa_e}{\kappa_D},$$

$$M_{21} = -M_{22} + \frac{\phi_0 \kappa_b}{\kappa_D}, \quad M_{22} = \frac{1}{2}\frac{\phi_0 \kappa_p}{\kappa_D}, \tag{35}$$

$$A = \frac{M_{11} + M_{21}}{M_{22} + M_{12}}, \quad \hat{S} = \frac{\rho_{ws} g_0 h \kappa_D \kappa_b (L^2 - R_1^2)}{\kappa_p R_p^2} = \frac{R_1^2}{R_p^2} S, \tag{36}$$

where a pipe radius $R_p \neq R_1$ leads to the replacement of S in the previous solution by $\hat{S}$. There is also a complex drag parameter

$$\lambda = (1 + i) \left\{ \left[\kappa_D + \frac{\phi_0 \kappa_p (\kappa_b + \kappa_e)}{\kappa_b (1 + \frac{4}{3}\bar{G})} \right] \frac{\rho_f g_0 h \phi_0 n}{2R_p^2} \right\}^{1/2}, \tag{37}$$

inversely proportional to R_p, with associated complex parameters

$$\Omega = \frac{I_0(\lambda R_1) K_1(\lambda L) + I_1(\lambda L) K_0(\lambda R_1)}{I_1(\lambda R_1) K_1(\lambda L) - I_1(\lambda L) K_1(\lambda R_1)}, \quad T = -\frac{\lambda(L^2 - R_1^2)}{2R_1}\Omega, \tag{38}$$

$$\alpha = A(1 - T) + M_{21} T / M_{22}, \quad \beta = [M_{12} A(1 - T) + M_{11} T] / M_{22}, \tag{39}$$

where I_0, I_1 and K_0, K_1 are modified Bessel functions of the first and second kind respectively (Magnus, Oberhettinger & Soni 1966).

The flux relation (30) becomes

$$2\kappa_D \rho_{ws} D + \kappa_p \rho_0 \hat{S} \{\hat{w}_0 - (1 - 2\phi_0)\hat{q}_0\} = 0. \tag{40}$$

Eliminating D from the well pressure expression (31) by (40) and applying the interface fluid pressure balance $(32)_1$ gives

$$(1 + \hat{S})\hat{w}_0 + \{\alpha - (1 - 2\phi_0)\hat{S}\}\hat{q}_0 - \hat{V} = \frac{2\kappa_D \rho_{ws} Y}{\kappa_p \rho_0}. \tag{41}$$

Eliminating P_w between $(32)_1$ and $(32)_2$ gives

$$\{\phi_0(M_{12} + M_{22}\hat{G}) - (1 - \phi_0)M_{22}\}\hat{w}_0 + M_{22}\{\phi_0(\beta - \hat{G}) - (1 - \phi_0)\alpha\}\hat{q}_0 - \{\phi_0(M_{12} - \bar{G}) - (1 - \phi_0)M_{22}\}\hat{V} = 0. \tag{42}$$

Finally, the overburden balance (33), neglecting the momentum term, becomes

$$\{M_{22}+M_{12}-\bar{G}\}\,\hat{w}_0+\{M_{11}+M_{21}+\bar{G}\}\,\hat{q}_0-\{M_{22}+M_{12}\}\,\hat{V}=\frac{\rho_r}{\rho_0}+\frac{1}{2H}. \tag{43}$$

The four complex equations (40)–(43) determine D, $\hat{w}_0$, $\hat{q}_0$ and $\hat{V}$ when all the coefficients, defined by the reservoir geometry and properties, are known, and from D we obtain the amplitude D_0 and phase lag τ. An explicit solution for D will now be derived.

4 Oscillation amplitude and phase lag

Solution of the equations (40)–(43) by algebraic expansion of the determinants does not yield a useful expression for D. However, equation (42), which expresses the proportionality between matrix and fluid partial radial stresses at the interface, gives an excellent approximate relation between $\hat{w}_0$ and $\hat{q}_0$ because of the relative magnitude of $\hat{G}$. Then equations (41) and (43) determine $\hat{w}_0$ and $\hat{q}_0$ explicitly and D is given by (40). Since M_{11} and M_{12} are order unity, and M_{22} and M_{12} are order unity if $\kappa_p = 0(\kappa_b/\phi_0)$ as anticipated, or order ϕ_0 if $\kappa_p = 0(\kappa_b)$ and ϕ_0 is small, we have

$$A = 0(1), \quad |\alpha| = \max 0(T, 1),$$
$$|\beta| = \max 0(T, 1) \text{ or } \max 0(T/\phi_0, 1/\phi_0). \tag{44}$$

Similarly, supposing $G \gtrsim 1/\kappa_b$,

$$\hat{G} \gtrsim \left(\frac{L}{R_1}\right)^2. \tag{45}$$

Now $|\lambda R_1| \ll 1$ for all feasible ranges of reservoir parameters, but $|\lambda L|$ may be small or exceed unity. Asymptotic results (see Appendix) show that

$$|T| \sim \begin{cases} 1, & |\lambda L| \ll 1, \\ -\tfrac{1}{2}\ln|\tfrac{1}{2}\lambda R_1|\,|\lambda L|^2, & |\lambda L| \gtrsim 1, \end{cases} \tag{46}$$

and hence

$$\frac{\hat{G}}{|T|} \sim \begin{cases} (L/R_1)^2, & |\lambda L| \ll 1, \\ 2/\{(-\ln|\tfrac{1}{2}\lambda R_1|)\,|\lambda R_1|^2\}, & |\lambda L| \gtrsim 1. \end{cases} \tag{47}$$

Since $R_1 = 0(10^{-2})$ and $L \gtrsim 10$ in practice, and $L = 10$ would represent a lower limit of the necessary strong inequality $(5)_1$, $\hat{G}/|T| \gtrsim 10^6$ for $|\lambda L| \ll 1$. Similarly, for $|\lambda L| \gtrsim 1$ corresponding to larger L and the upper ranges of ϕ_0 and n, numerical examples indicate that $|\lambda R_1| \lesssim 10^{-3}$, so again $\hat{G}/|T| \gtrsim 10^6$.

Thus, in all practical situations, supposing $\phi_0 \gtrsim 10^{-2}$,

$$\phi_0\hat{G} \gg 1, \quad \phi_0\hat{G} \gg |\alpha|, \quad \hat{G} \gg |\beta|, \tag{48}$$

where the ratios are at least 10^4, and generally much greater. In equation (42) therefore, the coefficients of $\hat{w}_0$ and $\hat{q}_0$ are respectively $\phi_0 M_{22}\hat{G}$ and $-\phi_0 M_{22}\hat{G}$, while the coefficient of $\hat{V}$ is of order M_{22}, so provided that $\hat{V}$ is of order $\hat{w}_0$ and $\hat{q}_0$, an excellent approximation is

$$\hat{w}_0 = \hat{q}_0. \tag{49}$$

Equation (43) confirms that $\hat{V}$ cannot exceed $\hat{w}_0$ and $\hat{q}_0$ in magnitude. Recalling the

definitions (29), the relation (49) implies

$$V_r^s|_{R=R_1} = 0; \tag{50}$$

that is, the matrix has no radial velocity at the interface and the flux into the well is entirely fluid. This result was not evident in the magnitude estimates made by Morland (1977). It does not follow in the plane flow solution, being associated with radial focusing. Eliminating $\hat{V}$ between (41) and (43) together with the relation (49) determines $\hat{w}_0 = \hat{q}_0$, and substitution in (40) gives

$$D = \frac{M_{22}\hat{S}(2\rho_r/\rho_{ws} + \rho_0/\rho_{ws}H) - 2\phi_0\hat{S}(M_{22}+M_{12})Y}{(M_{22}+M_{12})(\alpha + 2\phi_0\hat{S}) - (M_{11}+M_{21})}. \tag{51}$$

Using the definitions (24), (26) and (35)–(39) leads, after some manipulation, to an expression in terms of physical parameters:

$$\phi_0 D = \frac{B(\rho_r/\rho_{ws} + \rho_0/2\rho_{ws}H) - \phi_0 Y}{1-(i\Omega/2\lambda R_1)(\rho_f/\rho_{ws})n}, \tag{52}$$

$$B = \left\{1 + \frac{(1+\frac{4}{3}\bar{G})\kappa_D}{\nu\kappa_b} + \frac{\kappa_e}{\kappa_b}\right\}^{-1} = \left\{1 + \frac{(1+\frac{4}{3}\bar{G})(\kappa_f+\kappa_e)}{\nu\kappa_b} - \frac{\frac{4}{3}\bar{G}\kappa_e}{\kappa_b}\right\}^{-1}, <1. \tag{53}$$

It is now clear that the maximum magnitude of $\phi_0 D_0$ is unity, and this is reached only when

$$B = 0(1) \quad \text{and} \quad \left|\frac{\Omega}{\lambda R_1}\right| n \leqslant 0(1). \tag{54}$$

We suppose $\bar{G} = \kappa_b G \gtrsim 1$, so $B = 0(1)$ requires

$$\kappa_b \gtrsim \kappa_e \quad \text{and} \quad \nu\kappa_b \gtrsim \bar{G}\kappa_D \Rightarrow \nu(1+G\kappa_e) \gtrsim G(\kappa_f+\kappa_e). \tag{55}$$

The latter requires $\nu = 0(1)$ when $G\kappa_e \gtrsim G\kappa_f \gtrsim 1$ as assumed in our illustrations, and values of ν in the range 0.1–0.9 are adopted. Setting

$$x = \mathrm{Re}\left\{1 - \frac{i\Omega}{2\lambda R_1}\frac{\rho_f}{\rho_{ws}}n\right\}, \quad y = \mathrm{Im}\left\{-\frac{i\Omega}{2\lambda R_1}\frac{\rho_f}{\rho_{ws}}n\right\}, \tag{56}$$

the amplitude and phase lag are given by

$$D_0 = \frac{B(\rho_r/\rho_{ws} + \rho_0/2\rho_{ws}H) - \phi_0 Y}{\phi_0(x^2+y^2)^{1/2}}, \quad \tau = \tan^{-1}(y/x), \tag{57}$$

and it remains to estimate x and y in terms of n.

From (37), and applying (26),

$$\lambda^2 = i\phi_0 nK, \quad K = \frac{\rho_f g_0 h}{R_p^2}\left\{\kappa_D + \frac{\nu(\kappa_b+\kappa_e)}{1+\frac{4}{3}\bar{G}}\right\}, \tag{58}$$

and K is order unity for a practical range of parameters. Thus

$$|\lambda R_1| = R_1(\phi_0 nK)^{1/2} \ll 1, \quad |\lambda L| = L(\phi_0 nK)^{1/2}, \tag{59}$$

and $|\lambda L| \gtrsim 10(\phi_0 n)^{1/2}$ for $L \gtrsim 10$, allowing $|\lambda L| \sim 0.1$ when $\phi_0 = 0.01$, $n = 0.01$, $L = 10$.

With $\rho_{ws} = \rho_f$, asymptotic results (Appendix) show that

$$\begin{array}{ll} |\lambda L| \gtrsim 1 & |\lambda L| \ll 1 \\ x \sim 1 + \dfrac{\pi}{8} n, & 1 + \dfrac{n}{|\lambda L|^2} = 1 + \dfrac{1}{KL^2\phi_0}, \\ y \sim -\tfrac{1}{2} n \ln |\tfrac{1}{2}\lambda R_1|, & -\tfrac{1}{2} n \ln |R_1/L|, \end{array} \tag{60}$$

so that $x, y > 0$ as required for $0 < \tau < \pi/2$. Now $-\ln |R_1/L| \gtrsim 7$ for $R_1/L \leqslant 10^{-3}$, while $-\ln |\tfrac{1}{2}\lambda R_1|$ is approximately 11 for a wide range of parameters, so $y \lesssim 1$ when $n \lesssim 0.2$, which also implies $x = 0(1)$ since $KL^2\phi_0 \gtrsim 1$; this confirms the significant amplitude limit of the range (7). A phase lag exceeding 11° requires $\tan \tau \gtrsim 0.2$, and hence y a little greater since x is close to unity for significant amplitude, suggesting the lower bound $n \sim 0.04$ of the range (7). Though R_p influences n, λ is independent of R_p, so both D_0 and τ are influenced only through n and in particular the maximum magnitude of D_0 is not influenced by R_p.

While the asymptotic results (60) may be used to estimate D_0 and τ, these have been computed from the full expressions (57) using integral representations for the modified Bessel functions of complex argument (see Appendix). The important inverse problem of determining from (57) two reservoir properties from measured D_0 and τ will require interpolation from extensive tables or graphs of (D_0, τ) for a wide range of the various parameters, since all the parameters arise in the complex arguments of the Bessel functions. However, using the asymptotic results (60) leads to approximate non-linear algebraic equations from which two parameters may be estimated by direct numerical methods. The four compressibilities arise in the two combinations B and K, so if B and K are estimated, given ϕ_0 and n, then in principle any pair of compressibilities can be estimated given the other two and G. We now present the analysis for estimating the porosity ϕ_0 and permeability parameter n, and demonstrate the accuracy of the estimates by comparison with the direct calculations from (57).

Define

$$\bar{B} = \frac{B}{D_0}\left(\frac{\rho_r}{\rho_{ws}} + \frac{\rho_0}{2\rho_{ws}H}\right), \tag{61}$$

then with $B = 0(1)$, ϕ_0 small, as required for significant amplitude, (57) can be approximated to

$$x = \frac{\bar{B}\cos\tau}{\phi_0}, \quad y = \frac{\bar{B}\sin\tau}{\phi_0}, \tag{62}$$

where $\bar{B}$ and τ are given by the measured phase lag and oscillation amplitude. First consider $|\lambda L| \ll 1$, then the asymptotic results (60) give

$$\phi_0 = \bar{B}\cos\tau - \frac{1}{KL^2}, \tag{63}$$

independent of the n estimate, then

$$n = \frac{2\bar{B}\sin\tau}{\ln|L/R_1|\{\bar{B}\cos\tau - 1/KL^2\}}. \tag{64}$$

By (58) and these estimates, the estimated $|\lambda L| = L(K\phi_0 n)^{1/2}$, $\ll 1$ for validity of (63) and

(64). Now consider $|\lambda L| \gtrsim 1$, when (60) implies

$$\phi_0 = \frac{\bar{B}\cos\tau}{1+(\pi/8)n}, \quad n\ln|\tfrac{1}{2}\lambda R_1| + 2\left(1+\frac{\pi}{8}n\right)\tan\tau = 0, \tag{65}$$

where ϕ_0 has only a weak dependence on the estimated n when n is small. Eliminating λ by (58) and $(65)_1$ leads to the algebraic equation for n:

$$F(n) = n\left\{c_1 - \ln n + \ln\left(1+\frac{\pi}{8}n\right)\right\} - c_2 = 0, \tag{66}$$

where

$$c_1 = -\ln(\tfrac{1}{4}KR_1^2\bar{B}\cos\tau) - \frac{\pi}{2}\tan\tau, \quad c_2 = 4\tan\tau. \tag{67}$$

For practical values $c_1 \gg c_2 > 0$, so $F(0) = -c_2 < 0$, $F(1) = c_1 - c_2 + \ln(1+\pi/8) > 0$, and there is necessarily a root n on (0, 1). A standard numerical algorithm has determined a unique root on (0, 2) in all cases treated. Validity of (65) requires the estimated $L(K\phi_0 n)^{1/2} \gtrsim 1$. An alternative composite expansion has also been applied by using

$$x = 1 + \frac{\pi}{8}n + \frac{1}{KL^2\phi_0}, \quad y = -\tfrac{1}{2}n\ln|\tfrac{1}{2}\lambda R_1|, \tag{68}$$

which adds the small $|\lambda L|$ contribution to x for $|\lambda L| \gtrsim 1$. This may improve the $|\lambda L| \lesssim 1$ results without disturbing the $|\lambda L| \gg 1$ results when the extra term is negligible. With (68)

$$\phi_0 = \frac{\bar{B}\cos\tau - 1/KL^2}{1+(\pi/8)n}, \tag{69}$$

and n is the root of $F(n) = 0$ defined by (66) with

$$c_1 = -\ln\{\tfrac{1}{4}KR_1^2(\bar{B}\cos\tau - 1/KL^2)\} - \frac{\pi}{8}c_2, \quad c_2 = \frac{4\bar{B}\sin\tau}{\bar{B}\cos\tau - 1/KL^2}. \tag{70}$$

Comparisons and accuracy of the three sets of estimates are discussed with the numerical illustrations.

5 Numerical illustrations

It is clear that the full solution (57) is not significantly influenced by sensible variation of the parameters H, H_w, R_1, R_p, ρ_0, ρ_r, ρ_f (with $\rho_w \equiv \rho_f$ here), κ_f, κ_e and G, so we focus on the effects of varying L, h, κ_b, ν, ϕ_0 and n. Our calculations use the fixed values

$$\begin{aligned}
&\omega = 1.454\times10^{-4}\,\mathrm{s}^{-1}, \quad g_0 = 9.81\,\mathrm{m\,s}^{-2},\\
&H = 100, \quad H_w = 50, \quad R_1 = 0.01, \quad R_p = 0.01,\\
&(\rho_0, \rho_r, \rho_f) = (2, 2.7, 1)\times10^3\,\mathrm{kg\,m}^{-3},\\
&(\kappa_f, \kappa_e) = (4.3, 7)\times10^{-10}\,\mathrm{Pa}^{-1}, \quad G = 10^{10}\,\mathrm{Pa}.
\end{aligned} \tag{71}$$

The viscosity μ enters only through the parameter $\bar{k}$, and hence affects only required permeability k for a given value of n in the solution, and the tide magnitude $\tilde{g}$ ($\sim10^{-7}$) is simply a factor in the scaling $d \to D_0$. We have calculated $\phi_0 D_0$ and τ for the lateral extents

$L = 10$, 20, 30, 50, 70, 100 with $h = 10$ and 20 m, $\kappa_b = 10$ and $1 \times 10^{-10}\,\mathrm{Pa}^{-1}$, ϕ_0 over the range 0.01–0.1, and n over the range 0.01–1 which encompasses the estimated range of significance (7).

The first conclusion is that change of L above $L = 20$ has little effect on D_0 or τ, with the main influence shown near the lower limit $L = 10$. Detailed results will be presented only for $L = 50$ and 10. This means that the lateral extent L cannot be determined from the inverse solution. Next we find that τ is little changed by variation of $\nu = \phi_0\kappa_p/\kappa_b$, other parameters fixed, but that D_0 increases more than linearly with ν. Figs 3 and 4 show $\phi_0 D_0$

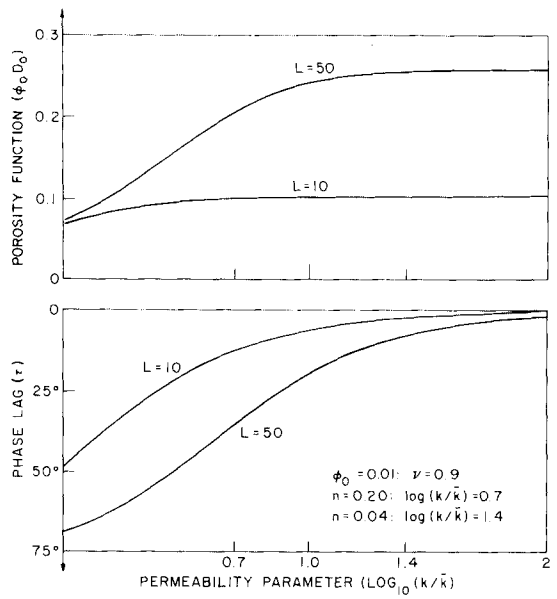

Figure 3. Influence of permeability on porosity and phase lag.

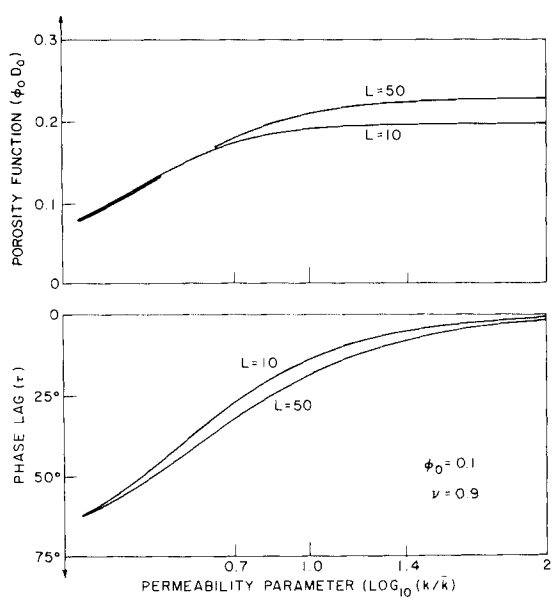

Figure 4. Influence of permeability on porosity and phase lag.

and τ as functions of $\log_{10}(k/\bar{k})$ for $\nu = 0.9$, $\phi_0 = 0.01$ and 0.1, at $L = 50$ and 10, and Figs 5 and 6 show the corresponding curves at $\nu = 0.7$, all with $h = 10$ m and $\kappa_b = 10^{-9}\,\mathrm{Pa}^{-1}$. The marked points $\log_{10}(k/\bar{k}) = 0.7$ and 1.4 correspond to $n = 0.2$ and 0.04 respectively, between which the combination of significant D_0 and significant τ was estimated to lie (7), confirmed by these illustrations. $\phi_0 D_0$ increases with k, but is nearly uniform by $n = 0.01$. It is clear that $\phi_0 D_0$ is not significantly changed between $\phi_0 = 0.01$ and 0.1 at $L = 50$, so D_0 is roughly proportional to ϕ_0^{-1}, but increases with increase of ϕ_0 at $L = 10$. However, $L = 50$ provides the greater value of $\phi_0 D_0$ for both values of ϕ_0, and hence the greater D_0. Similarly, τ is only

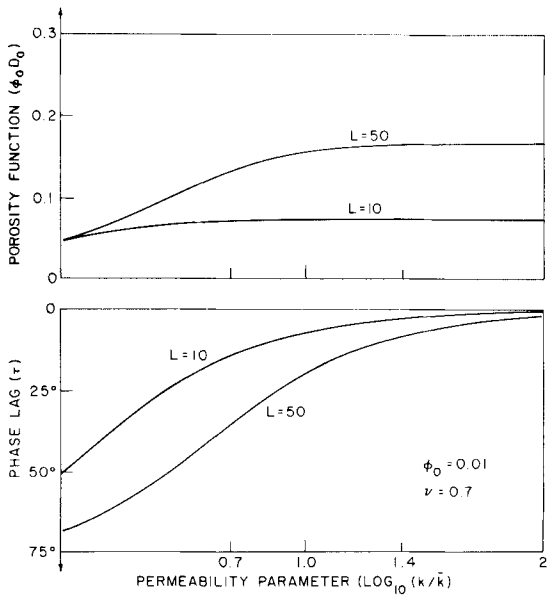

Figure 5. Influence of permeability on porosity and phase lag.

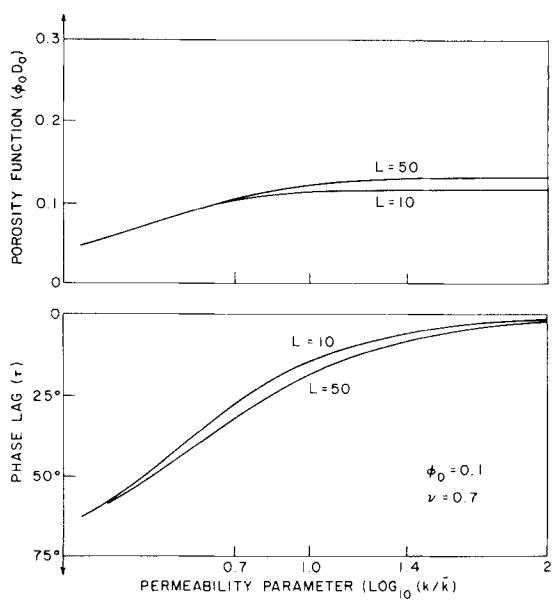

Figure 6. Influence of permeability on porosity and phase lag.

Table 1. Influence of h and κ_b on $\phi_0 D_0$ and τ.

	n	0.2		0.1		0.05	
L	ϕ_0	$\phi_0 D_0$	τ_0^0	$\phi_0 D_0$	τ_0^0	$\phi_0 D_0$	τ_0^0
		$h = 10\,\text{m}$, $\kappa_b = 10^{-9}\,\text{Pa}^{-1}$					
50	0·01	0·206	35·4	0·242	19·9	0·254	10·3
10	0·01	0·100	12·9	0·102	6·6	0·103	3·3
50	0·1	0·179	32·7	0·209	19·4	0·222	10·6
10	0·1	0·173	27·6	0·190	14·7	0·195	7·5
		$h = 20\,\text{m}$, $\kappa_b = 10^{-9}\,\text{Pa}^{-1}$					
50	0·01	0·209	35·5	0·247	20·3	0·261	10·6
10	0·01	0·142	18·5	0·148	9·5	0·149	4·8
50	0·1	0·182	31·4	0·210	18·5	0·222	10·1
10	0·1	0·182	29·1	0·203	15·8	0·210	8·1
		$h = 10\,\text{m}$, $\kappa_b = 10^{-10}\,\text{Pa}^{-1}$					
50	0·01	0·094	35·6	0·110	20·1	0·116	10·5
10	0·01	0·053	15·2	0·054	7·8	0·055	3·9
50	0·1	0·062	32·2	0·072	19·0	0·076	10·4
10	0·1	0·061	28·4	0·067	15·3	0·069	7·8

influenced strongly by ϕ_0 at $L = 10$. Generally τ decreases as L decreases, and shows marked decrease as k increases as expected – decreasing phase lag as the drag decreases.

The influences of h and κ_b are demonstrated by the selection of values shown in Table 1 for the pairs $h = 10\,\text{m}$, $\kappa_b = 10^{-9}\,\text{Pa}^{-1}$; $h = 20\,\text{m}$, $\kappa_b = 10^{-9}\,\text{Pa}^{-1}$; $h = 10\,\text{m}$, $\kappa_b = 10^{-10}\,\text{Pa}^{-1}$; with $\nu = 0.9$. First we see that both $\phi_0 D_0$ and τ increase with h at $L = 10$ and $\phi_0 = 0.01$, but show little change at $L = 50$ or 10 and $\phi_0 = 0.1$. So h does not influence the maximum amplitude that can be attained significantly, as evident in equation $(57)_1$; the inverse solution cannot determine h from measured D_0 and τ. However, the decrease of κ_b by a factor 10, from a value exceeding κ_f and κ_e to one below, yields a significant decrease in $\phi_0 D_0$, arising from the term $(\kappa_f + \kappa_e)/\nu\kappa_b$ in B^{-1}, (53), recalling $\bar{G} = \kappa_b G$. τ is not appreciably changed at any L, ϕ_0 combination since the solution is not strongly sensitive to the modest variation of λ with change of κ_b (58).

Finally, we examine the asymptotic estimates of ϕ_0 and n when D_0 and τ are known, by using values of D_0, τ, calculated by (57) for a range of given ϕ_0 and n values, and comparing the estimates with the given values. Let n_1, n_2, n_3 be the estimates of n from (64), $|\lambda L| \ll 1$, from (66), (67), $|\lambda L| \gtrsim 1$, and from (66), (70), the alternative $|\lambda L| \gtrsim 1$ expansion, with ϕ_1, ϕ_2, ϕ_3 the corresponding estimates of ϕ_0. Table 2 shows a selection of comparisons using $h = 10\,\text{m}$, $\kappa_b = 10^{-9}\,\text{Pa}^{-1}$, $\nu = 0.9$, for $L = 50$ and 10, with the respective values of $|\lambda L|$. An asterisk * in the $|\lambda L|$ column indicates that both n_1 and ϕ_1 are better estimates than n_2 and ϕ_2, and ϕ_1 is shown in the 'ϕ_1 or ϕ_2' column, these results fall in the range $|\lambda L| \leqslant 1.73$. The non-* results have both n_2 and ϕ_2 better than n_1 and ϕ_1. A dagger † in the $|\lambda L|$ column indicates that both n_3 and ϕ_3 are better estimates than n_2 and ϕ_2 (and n_1 and ϕ_1), corresponding to the range $|\lambda L| \geqslant 4.31$. A dagger † in the n_3 column indicates that n_3 is a better estimate than n_2 (and n_1), but ϕ_3 is a worse estimate than ϕ_2, corresponding to the range $1.54 \leqslant |\lambda L| \leqslant 3.86$. At $|\lambda L| = 1.54$, n_3 is a better estimate than n_1 as well as n_2, but ϕ_3 is not as good as ϕ_1, and $n_3 = n_1$ at $|\lambda L| = 1.22$. A rough guide suggested by these results, based on estimated values of $|\lambda L|$ from the inverse solutions, is to adopt the following estimates

$\lvert\lambda L\rvert < 1.9$	$1.9 \leqslant \lvert\lambda L\rvert \leqslant 4$	$\lvert\lambda L\rvert > 4$
n_1, ϕ_1	n_3, ϕ_2	n_3, ϕ_3

(72)

Table 2. Estimates of ϕ_0 and n by asymptotic inversions.

L	$\lvert\lambda L\rvert$	ϕ_0	ϕ_1 or ϕ_2	ϕ_3	n	n_1	n_2	n_3
50	2·44	0·01	0·0100	0·0093	0·4	0·3332	0·3652	0·3914‡
10	0·49*	0·01	0·0100		0·4	0·3553	0·1131	0·3266
50	1·93	0·01	0·0101	0·0094	0·25	0·2193	0·2215	0·2372‡
10	0·39*	0·01	0·0100		0·25	0·2226	0·0675	0·1892
50	1·22*	0·01	0·0101		0·1	0·0906	0·0821	0·0878
10	0·24*	0·01	0·0100		0·1	0·0891	0·0250	0·0686
50	0·77	0·01	0·0100		0·04	0·0364	0·0306	0·0327
10	0·15*	0·01	0·0100		0·04	0·0357	0·0097	0·0254
50	5·46‡	0·05	0·0507	0·0500	0·4	0·2848	0·3624	0·3673
10	1·09*	0·05	0·0509		0·4	0·3502	0·2633	0·3626
50	4·31‡	0·05	0·0504	0·0497	0·25	0·1943	0·2287	0·2318
10	0·86*	0·05	0·0503		0·25	0·2213	0·1544	0·2102
50	2·73	0·05	0·0500	0·0493	0·1	0·0871	0·0919	0·0932‡
10	0·55*	0·05	0·0501		0·1	0·0890	0·0563	0·0758
50	1·73*	0·05	0·0502		0·04	0·0362	0·0353	0·0358
10	0·35*	0·05	0·0500		0·04	0·0357	0·0208	0·0290
50	7·72‡	0·1	0·1014	0·1007	0·4	0·2690	0·3606	0·3630
10	1·54*	0·1	0·1034	0·0901	0·4	0·3436	0·3166	0·3756†
50	6·10‡	0·1	0·1008	0·1002	0·25	0·1835	0·2273	0·2298
10	1·22*	0·1	0·1013	0·0933	0·25	0·2196	0·1861	0·2196‡
50	3·86	0·1	0·1003	0·0996	0·1	0·0830	0·0921	0·0927†
10	0·77*	0·1	0·1002		0·1	0·0889	0·0676	0·0793
50	2·44	0·1	0·1000	0·0993	0·04	0·0356	0·0365	0·0368‡
10	0·49*	0·1	0·1000		0·04	0·0356	0·0250	0·0293

Note that n_2 is never the best estimate of n. From the numerical examples the worst error in n is 14 per cent, using n_1 at $|\lambda L| = 1.54$, while the worst error in ϕ_0 is 5 per cent using ϕ_1 at $|\lambda L| = 1.09$, with much better estimates in many cases. Overall, the estimates (72) give very satisfactory agreement with the correct values of n and ϕ_0.

6 Concluding remarks

The axisymmetric elastic matrix model analysed here allows explicit solutions for the amplitude and phase lag of well fluid oscillations arising from earth tide induced motions in a deep reservoir. Amplitudes of order 1 cm can be attained only when the bulk compressibility κ_b exceeds the fluid compressibility κ_f and effective rock compressibility κ_e, and when the formation compaction $\kappa_p = 0(\kappa_b/\phi_0)$ and the fluid volume fraction ϕ_0 is of order 0.01. The solutions are relatively insensitive to sensible changes of the lateral extent and thickness of the reservoir, but depend strongly on the fluid volume fraction and on the permeability k through a dimensionless parameter n relating permeability to the fluid viscosity μ and density ρ_f, tide frequency ω, layer thickness h, and well (or pipe) radius $r_1(r_p)$. A range of n yielding a combination of significant amplitude and significant phase lag is obtained. Asymptotic expansions allows inverse solutions to determine ϕ_0 and n from measured amplitude and phase lag, given the other reservoir properties, and numerical examples show that good accuracy is obtained.

A packed well pipe radius r_p enters only through the parameter n, so has little influence on the amplitude once a significant amplitude has been attained. However, estimates of n from D_0, τ_0 values observed for different r_p in the same well-reservoir configuration should

confirm the proportionality, (6),

$$\frac{g_0 n}{\omega r_p^2} = \frac{\mu}{\rho_f h k}, \tag{73}$$

and determine one of the parameters μ, ρ_f, h, k in the right-hand constant, given the other three, Well packing can therefore provide some further information about the reservoir properties.

It is reasonable to suppose that the vanishing of the matrix velocity at the well interface will extend to non-symmetric configurations and to multi-well configurations involving interactions. Coupled with the successful vertical-horizontal separation (Morland 1977), this should provide a useful simplification in seeking numerical solutions of the resulting two-dimensional horizontal balance equations. Weak interactions of two wells far apart on the reservoir thickness scale may even yield to asymptotic methods. The incorporation of a perforated pipe in contrast to the open interface analysed here is the important extension, and now a vanishing matrix velocity at the wall is reinforced, and provides a starting point for the new interface conditions.

References

Amyx, J. W., Bass, B. M. & Whiting, R. L., 1960. *Petroleum Reservoir Engineering*, McGraw-Hill, New York.

Biot, M. A. & Willis, D. G., 1957. The elastic coefficients of the theory of consolidation, *J. appl. Mech.*, **79**, 594–601.

Bodvarsson, G., 1970. Confined fluids as strain meters, *J. geophys. Res.*, **75**, 2711–2718.

Bredehoeft, J. D., 1967. Well-aquifer systems and earth tides, *J. geophys. Res.*, **72**, 3075–3087.

Cooper, H. H., Bredehoeft, J. D., Papadopulos, I. S. & Bennett, R. R., 1965. The response of well-aquifer systems to seismic waves, *J. geophys. Res.*, **70**, 3915–3926.

Geertsma, J., 1957. The effect of fluid pressure decline on volumetric changes of porous rocks, *Petrol. Trans. AIME*, **210**, 331–340.

Magnus, W., Oberhettinger, F. & Soni, R. P., 1966. *Formulas and Theorems for the Special Functions of Mathematical Physics*, Springer-Verlag, Berlin.

Marine, I. W., 1975. Water level fluctuations due to earth tides in a well pumping from slightly fractured crystalline rock, *Wat, Resour. Res.*, **11**, 165–173.

Melchior, P., 1983. *The Tides of the Planet Earth*, 2nd edn, Pergamon Press, Oxford.

Morland, L. W., 1972. A simple constitutive theory for a fluid-saturated porous solid, *J. geophys. Res.*, **77**, 890–900.

Morland, L. W., 1975. Effective stress in mixture theory, *Arch. Mech.*, **27**, 883–887.

Morland, L. W., 1977. Earth tide effects on flows in horizontal permeable elastic layers connected to wells, *Geophys. J. R. astr. Soc.*, **51**, 371–385.

Morland, L. W., 1978. A theory of slow fluid flow through a porous thermoelastic matrix, *Geophys. J. R. astr. Soc.*, **55**, 393–410.

Rhoades, G. H. & Robinson, E. S., 1979. Determination of aquifer parameters from well tides, *J. geophys. Res.*, **84**, 6071–6082.

Rinehart, J. S., 1972. Fluctuations in geyser activity caused by variations in earth tidal forces, barometric pressure and tectonic stresses, *J. geophys. Res.*, **77**, 342–350.

Rinehart, J. S., 1976. Influence of tidal strain on geophysical phenomena, *Proc. seventh int. Symp. on Earth Tides*, pp. 181–185, 1973, Budapest, Akademiai Kiado.

Rinehart, J. S., 1975. Alterations of flow characteristics within geothermal areas by tidal forces, *Rep. CUMER 75–6*, Department of Mechanical Engineering, University of Colorado, Boulder, Colorado, USA.

Robinson, E. S. & Bell, R. T., 1971. Tides in confined well-aquifer systems, *J. geophys. Res.*, **76**, 1857–1869.

Sperling, K., 1953. Is there a tidal influence on petroleum production? *Erdöl Kohle*, **6**, 446–449.

Appendix A: Bessel function formulae

The basic results for the modified Bessel functions of the first and second kind, $I_0(z)$, $I_1(z)$ and $K_0(z)$, $K_1(z)$, respectively, where z is a complex variable, are given by Magnus *et al.* (1966). Numerical evaluations of $I_0(z)$, $I_1(z)$, were made from the integral representations

$$I_0(z) = \frac{1}{\pi}\int_0^{\pi/2} \exp(-z\sin\theta)\,d\theta + \frac{\exp(z)}{\pi}\int_0^{\pi/2} \exp[-z(1-\sin\phi)]\,d\phi, \tag{A1}$$

$$I_1(z) = \frac{z}{\pi}\int_0^{\pi/2} \cos^2\theta \exp(-z\sin\theta)\,d\theta + \frac{z\exp(z)}{\pi}\int_0^{\pi/2} \cos^2\phi \exp[-z(1-\sin\phi)]\,d\phi, \tag{A2}$$

which provide high accuracy using a simple 5-point quadrature rule for all z such that $\mathrm{Re}(z) > 0$. Recall that $\mathrm{Re}(\lambda) > 0$. Similarly,

$$K_0(z) = \int_0^1 \exp[-z(s + 1/s)]\frac{ds}{s} \tag{A3}$$

is accurate for $\mathrm{Re}(z) > 0$ and $|z| \geqslant 0.2$, while the asymptotic result

$$K_0(z) = -\gamma - I_0(z)\ln(z/2) + \tfrac{1}{4}(1-\gamma)z^2 + z^{-6}(1.5-\gamma)z^4 + 0(z^6), \qquad \gamma = 0.57722, \tag{A4}$$

is excellent for $|z| < 0.2$. Finally, $K_1(z)$ is evaluated from the identity

$$I_0(z)K_1(z) + I_1(z)K_0(z) = \frac{1}{z}. \tag{A5}$$

The asymptotic formulae for $|z| \ll 1$ are (A4) and

$$I_0(z) = 1 + \tfrac{1}{4}z^2 + 0(z^4),\ I_1(z) = \tfrac{1}{2}z + \tfrac{1}{4}z^3 + 0(z^5),\ K_1(z) = \frac{1}{z} + \tfrac{1}{2}z\ln(z/2) + 0(z). \tag{A6}$$

The asymptotic results (46), (47) and (60), follow from the expansion for Ω, (38), when $|\lambda R_1| \ll 1$,

$$\Omega = \lambda R_1 \ln(\tfrac{1}{2}\lambda R_1) - \lambda R_1 K_1(\lambda L)/I_1(\lambda L) + 0(\lambda R_1), \tag{A7}$$

where $(R_1/L)^2$ is neglected in comparison with unity when $|\lambda L| \ll 1$. Thus

$$|\lambda R_1| \ll 1, \quad |\lambda L| \gtrsim 1: \quad \Omega \sim \lambda R_1 \ln(\tfrac{1}{2}\lambda R_1), \tag{A8}$$

$$|\lambda R_1| \ll 1, \quad |\lambda L| \ll 1, \quad |R_1/L| \ll 1: \quad \Omega \sim -\frac{2\lambda R_1}{(\lambda L)^2} - \lambda R_1 \ln(L/R_1). \tag{A9}$$

Appendix B: list of symbols

A	dimensionless parameter related to reservoir elasticity (36)
B	dimensionless parameter related to reservoir elasticity (53)
d	well fluid surface displacement
D	complex dimensionless displacement of well fluid surface (3)
D_0	magnitude of D (2)
g	gravity acceleration
g_0	mean gravity acceleration

$\tilde{g}$ dimensionless amplitude of gravity variation (1)
G matrix shear modulus
$\bar{G}$ dimensionless shear modulus (34)
$\hat{G}$ dimensionless modulus related to $\bar{G}$ and geometry (34)
h reservoir thickness
h_r overburden thickness, $H = h_r/h$
h_w height of well fluid surface above reservoir, $H_w = h_w/h$
$\bar{k}$ permeability unit defined by configuration and gravity variation (6)
k permeability of matrix, $n = \bar{k}/k$
l reservoir radius, $L = l/h$
p^f partial pressure increment in fluid
${}^E p^f$ intrinsic pressure increment in fluid
p^s partial pressure increment in matrix
${}^E p^s$ intrinsic pressure increment in matrix
P complex amplitude of dimensionless partial fluid pressure increment (28)
P_w complex amplitude of dimensionless well fluid pressure increment at reservoir level (31)
$\hat{q}_0$ difference of scaled radial velocity increments of fluid and matrix at well interface (29)
r_1 radius of well, $R_1 = r_1/h$
r_p radius of well pipe, $R_p = r_p/h$
S dimensionless parameter related to reservoir geometry and elasticity (36)
T complex parameter related to geometry and drag (38)
$\mathbf{v}^f$ velocity increment of fluid
$\mathbf{v}^s$ velocity increment of matrix
$\mathbf{V}^f$ complex amplitude of dimensionless velocity increment of fluid (28)
$\mathbf{V}^s$ complex amplitude of dimensionless velocity increment of matrix (28)
V complex amplitude of dimensionless vertical velocity of overburden, $\hat{V} = 2V/H$
V_r^f radial component of $\mathbf{V}^f$ at well interface
V_r^s radial component of $\mathbf{V}^s$ at well interface
$\hat{w}_0$ sum of scaled radial velocity increments of fluid and matrix at well interface (29)
Y dimensionless height related to weight of well fluid column (31)
α complex parameter related to T and reservoir elasticity (39)
β complex parameter related to T and reservoir elasticity (39)
δ unjacketed compressibility (18)
ϵ^f partial dilatation increment in fluid
${}^E\epsilon^f$ intrinsic dilatation increment in fluid
ϵ^s partial dilatation increment in matrix
${}^E\epsilon^s$ intrinsic dilatation increment in matrix
κ_b bulk compressibility of reservoir at constant pore pressure (15)
κ_e effective rock compressibility of reservoir (21)
κ_f intrinsic fluid compressibility at reservoir conditions
κ_p formation compaction of reservoir (19)
κ_s intrinsic matrix compressibility at reservoir conditions,
κ_D see (24), ν see (26)
λ complex drag parameter (37)
μ reservoir fluid viscosity
ρ_f intrinsic reservoir fluid density
ρ_r density of overburden

ρ_0	reservoir density in equilibrium
ρ_{w0}	well fluid density at reservoir level
ρ_{ws}	well fluid density at surface
$\boldsymbol{\sigma}^s$	partial stress increment in matrix
$^E\boldsymbol{\sigma}^s$	intrinsic stress increment in matrix
σ_{rr}	radial component of $\boldsymbol{\sigma}^s$
σ_{zz}	vertical component of $\boldsymbol{\sigma}^s$
Σ_{rr}	complex amplitude of dimensionless radial stress (28)
Σ_{zz}	complex amplitude of dimensionless vertical stress (28)
τ	phase lag of well fluid level oscillation, $\omega\Delta t$ (3)
ϕ	matrix porosity
ϕ_0	matrix porosity in equilibrium
ω	gravity variation frequency
Ω	complex parameter related to geometry and drag (38)